Military Technical College
Kobry El-Kobbah,
Cairo, Egypt

8th International Conference
on Electrical Engineering
ICEENG 2012

Extracting High Quality Information From Under Sampled Images with Relative Motion Blur Using Non-blind Restoration Techniques: A Survey

By

W. M. Hendawy* G. I. Salama** H. A. Hussein** K. I. Hassanien*

Abstract:

Image degraded due motion blur is an ill-posed problem that still attracts many researchers to participate in solving such problem. The degraded image might suffer linear or nonlinear motion blur. It may also be due to the camera motion (spatial space invariant) or due to the motion of the target to be captured (spatially space variant). This paper focuses on images degraded due to linear motion blur due to the camera motion. A survey was done over several kernel estimation techniques such as ***Cepstral*** and ***Sinc function*** whom are classified under parameter estimation approach, and Fergus[1] and Krishnan[2] techniques who are classified under MAP_h (Maximum A Posteriori over the kernel *h*) estimation approach. Experiments were applied over images samples suffering a synthetic blur and restored with several image restoration algorithms.

Keywords:

Image restoration, motion blur and kernel estimation.

* Technical Research Department
** Egyptian Armed Forces

1. Introduction:

Images are produced to record or display useful information. Due to imperfections in the imaging and capturing process, the recorded image invariably represents a degraded version of the original scene.

Overcoming these imperfections is crucial to many of the subsequent image processing tasks. There exists a wide range of different degradations that have to be taken into account, for instance, noise, geometrical degradations, illumination and color imperfections (under- or over- exposure, saturation), and blur.

There are several types of **blur** that may cause the degradation of a captured image, e.g., lenses imperfections, atmospheric turbulence, and object motion. Degradation can be either **spatially invariant** or **variant**.

In spatially-invariant degradation, all the pixels in the image are affected exactly. Poor lens focus or motion of the camera, are the main cause for such degradation. The pixels' locations aren't affected by this distortion.

In spatially-variant degradations, the recorded pixel values are dependent on the spatial location. So they are more difficult to model than degradations that do not change with location. Examples of these types are linear, non-linear and spiral motion blur.

This paper concentrates on removing blurriness introduced due to **linear shift invariant motion** from recorded sampled (spatially discrete) images. The standard model of the degraded image is given by this fundamental imaging equation:

$$g = f \otimes h + n \tag{1}$$

This paper is organized as follows: section (2) introduces a brief about different types of image restoration frameworks followed that are used to recover a latent image from its degraded version. Section (3) discusses two major approaches of kernel estimation, parameter estimation approach and MAP estimation approach. Section (4) discusses some image restoration methods. Section (5) reviews the related work of some researchers discussed that type of image degradation and what they produced in that field to overcome blurriness due to shift invariant motion. Section (6) includes discussions and experimental results gained from testing different image restoration algorithms with different kernel estimation approaches over some image sample in different circumstances. Section (7) introduces a conclusion of this paper and what is expected to be performed in the future.

2. Image Restoration Frameworks:

The field of ***image restoration*** (sometimes referred to as image de-blurring or image de-convolution) is concerned with the reconstruction or estimation of the uncorrupted image from a blurred and noisy one. Essentially, it tries to perform an operation on the image that is the inverse of the imperfections in the image formation system.
Image restoration can be classified into two major class, blind image restoration/de-convolution and non-blind image restoration.
When the attributes of the imperfect imaging system can be estimated before the process of de-blurred/latent image estimation process, this combination of image restoration and blur identification is can be noted as ***non-blind image de-convolution*** [3]. Figure (1-a) describes the framework of the non-blind image restoration. The characteristics of the degrading/blurring function (kernel) and the noise are assumed to be known ***a priori.*** With the help of an image restoration algorithm, the latent image can be estimated.
In practical situations, however, one may not be able to obtain this information directly from the image formation process. When the attributes are required to be estimated in the same time with the de-blurred/latent image, the combination of image restoration and blur identification is often referred to as ***blind image restoration/de-convolution***. Blind image restoration is the process of estimating the latent image and the kernel simultaneously with the help of some available prior knowledge about the degraded image and the imaging system [4]. Figure (1-b) describes the framework of the blind image restoration. Both prior knowledge about the attributes of the imperfect imaging system and an initializing state of the kernel have to be taken in consideration before the estimation process. A recursive process is applied in order to estimate the blurring function (kernel) and the latent image until a certain threshold is reached. The output of this process is the required latent image and the kernel caused the degradation.

3. Kernel Estimation:

The linear shift invariant motion blur is produce as a result of the translation of the recording instrument (camera) at a constant velocity which results a movement of the recorded pixel with distance l away of its right location with an angle θ computed from the horizontal axis and degrading the recorded image with one-dimensional distortion.
There exist different approaches to estimate the kernel. Some of these approaches depend on calculating the kernel parameters, the angle θ and the displacement l [5]. But recently published papers exploit the degraded image in order to estimate the kernel by means of mathematical approaches (e.g. a maximum a posteriori probability MAP) [2][6][7]. This section introduces some of the well-known approaches used in kernel estimation.

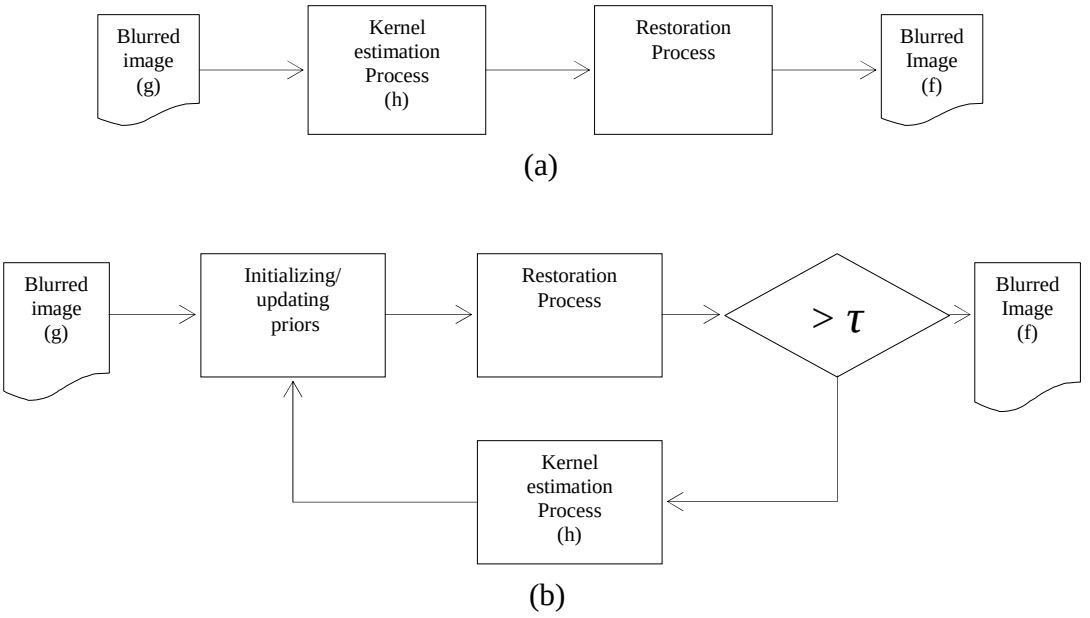

Figure (1): *Image restoration framework: (a) Framework of the non-blind image restoration/de-convolution process. (b) Framework of the blind image restoration process, τ=threshold.*

In parameter estimation approach, the ***Sinc function*** and ***Cepstral method***'s algorithms are discussed as an example for calculating the angle of motion and its displacement. The algorithms produced by ***Fergus*** [1] and ***Krishnan*** [2] also introduced as examples of MAP estimation approach.

3.1. Parameter Estimation:

Early researches [5][8][9] assumed that since the blur causing the degradation is due to a linear motion and this kind of blur is motion invariants blur, thus by estimating the angle of the motion and the displacement of this motion we can estimate the kernel, which is an important term in solving the degradation problem [5]. Eq. (2) shows how the kernel can be computed with the help of angle θ and displacement L. Several forms of solutions were built on that equation.

$$h(x,y;L,\theta)=\begin{cases}\dfrac{1}{L} & \text{if } \sqrt{x^2+y^2}\le\dfrac{L}{2}, \dfrac{x}{y}=-\tan\theta \\ 0 & \text{elsewhere}\end{cases} \quad (2)$$

One of these forms is the ***Sinc function*** algorithm [8]. This algorithm was built depending on the regular patterns of zeros found in the Fourier spectrum of the image degraded by linear motion. Figure (2) shows the Fourier spectrum of the blurred image and the used detecting function. This algorithm detects those patterns by minimizing the correlation between the Fourier spectrum of the observed image and a function detects the place of those patterns.

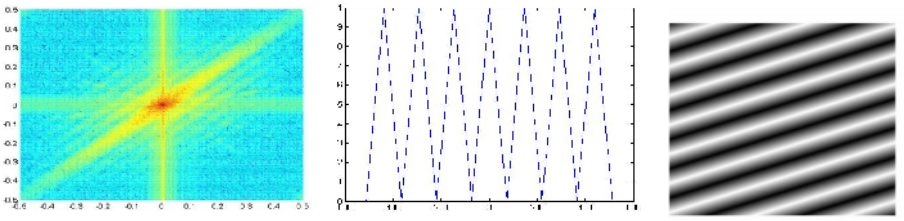

(a) (b) (c)

Figure (2): Sinc function estimation method *(a) The Fourier spectrum of the blurred images (vertical view). (b) The* ***Sinc function*** *(horizontal view). (c) The* ***Sinc function*** *(vertical view).*

Another algorithm was introduced based on eq. (2). This algorithm based on the ***Cepstrum*** of the blurred image. The Cepstrum of the blurred image has large peaks with negative values [9][10]. By calculating the distance between those two peaks and the angle of the line connecting between those peaks, we can obtain the parameters used in computing the kernel. Figure (3) shows the Cepstrum of an image blurred at length 20 and $\theta = 30$. In (a) we see the two prominent negative peaks and in (b) the line through these two peaks appear to have an angle of 30 degrees. This kernel estimation technique is very sensitive to noise. If the noise level of the blurred image is not too high, two peaks will be easily noticed in the Cepstrum, as show in Figure (3). In order to compute the angle of motion blur, a straight line will be drawn from the origin to the first negative peak. The angle of motion blur is approximated by the inverse tangent of the slope of this line.

3.2 MAP Estimation:

One of the well-known and simplest workarounds to blind restoration/de-convolution is a MAP estimation of the latent image *f* and kernel *h*. A pair *f, h* is been searched for maximizing the posterior probability given the observed image *g*. The resulted pair is expected to satisfy the convolution constraints up to noise, and will have sparse derivatives, that is, minimize the sum of derivatives. Having such a good prior will lead

to solve blind de-convolution, and it is expected that optimizing a $MAP_{f,h}$ score will provide the desired sharp image.

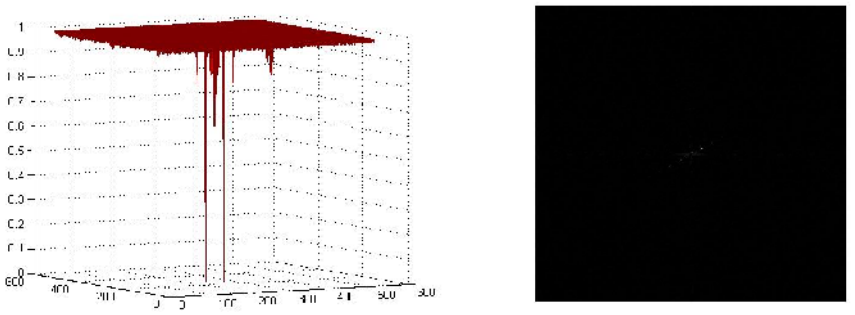

(a) (b)

Figure (3): Cepstral estimation method: *the cepstrum of an blurred image (a) The two noticeable peaks. (b) The two peaks in vertical view showing a line deviated from the x-axis with angle=30.*

Unfortunately, Real images contain a lot of low resolution details which acts like impulse signals. The contrast is reduced by blur. When a natural image is blurred, this blurriness reduces the total derivatives contrast and therefore a blurred image signal achieves a higher probability than a sharp one. The proof of this fact will be explained in section 5, which also explains why the use of MAP_h becomes for fruitful than $MAP_{f,h}$.

In $MAP_{f,h}$, the number of the unknown information is higher than the number of the known information. This came from that the needed latent image *f*, which is in the same size of the blurred image *g*, plus the kernel *h* are formatting the unknown information. Fergus *et al.* [1] produced an algorithm that used the blurred image Gaussian gradients as a prior for the restoration process. Figure (4) shows the histogram of the gradients for both blurred image and the un-blurred image. It also shows the parametric model they built to be used as a prior in kernel estimating process.

They estimate the kernel with the help of this prior and the blurred image *g* with size NxM. The number of the unknown information is much less than the known information. This helps to produce a better and very close to the blurring function caused the degradation. With the help of MAP_h approach, they overcame the leakage in information that was led because of the higher number of unknowns.

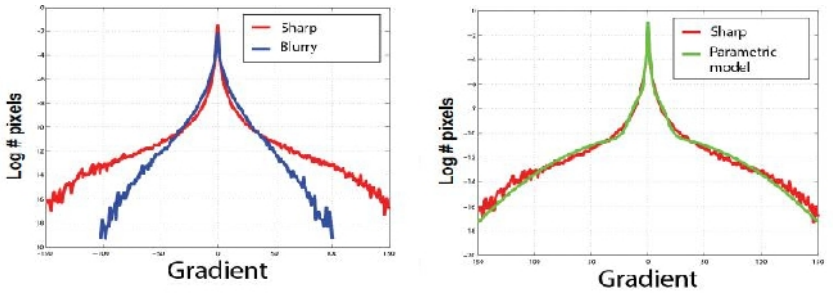

(a) (b)

Figure (4): *Gradient distributions (a) Sharp (un-blurred) and blurry gradient distribution. (b) Parametric model of mixture of Gaussians versus the sharp gradient distribution.*

Krishnan *et al*. [2] used the same concept of using MAP_h approach to build their own model. They replaced the image Gaussian gradient priors with hyper-Laplacian image priors. They used this prior to achieve kernel estimation to be as an input of any restoration algorithm to gain the latent image [2].

4 Restoration Methods:

After showing how the kernel of the blur is computed. Hence, it will be needed to estimate the original image *f* with the help of the known terms, the blurred image *g* and the blur kernel *h*.

A number of methods can be used for removing the blur from the recorded (blurred) image *g* using the computed kernel:

- Iterative Least Squares Method.
- Iterative Constrained Least Squares Method.
- Iterative L^2 Norm method.
- Iterative Total Variation Method.

The simplest form of an iterative restoration process will take the form as [11]:

$$f_{k+1} = f_k + \beta\Phi(f_k) \tag{3}$$

Where β controls the convergence as well as the rate of convergence of the iteration and $0< \beta <2$.

Eq. (3) can be re-written in the following form:

$$f_{k+1} = \beta g + (I - \beta h) f_k \tag{4}$$

4.1 Least Squares method:

One of the most famous basic filters used for de-blurring degraded images due to motion is the **inverse filter**. This filter suffers of the instability because it is unsuccessful when dealing with noise. This instability came from the sensitivity of the inverse filter to overcome the presence of noise in the degraded image. A number of restoration filters have been developed; these are collectively called least-squares filters.

According to the least squares approach, a solution to eq. (1) can be derived by minimizing $\|g - hf\|^2$. To get that minimal, it is necessary to have the gradient of $\|g - hf\|^2$ with respect to *f* is equal to zero as follows [12]:

$$\hat{f}_{LS} = argmin_f \|g - h \cdot f\|_2^2 \tag{5}$$

As a conclusion of both eq. (4), (5) then the iterative least square will take the following form [11]:

$$f_{k+1} = \beta h^T g + (I - \beta h^T h) f_k \tag{6}$$

4.2 Constrained Least Squares Method:

The method of 'constrained least-square' can be defined as the optimization of some criterion of goodness or quality of image subject to the constraint that residual norm between the image and the re-degraded estimated image be equal to the norm of the noise vector[13].

The image restoration problem is an ill-posed problem, which means that matrix *h* is ill conditioned. A **regularization method** replaces an ill-posed problem by a well-posed problem, whose solution is an acceptable approximation to the solution of the ill-posed problem [14]. Most regularization approaches transform the original inverse problem into a constrained optimization problem. That means, a functional has to be optimized with respect to the original image, and possibly other parameters.

By using the necessary condition for optimality, the gradient of the functional with respect to the original image is set equal to zero, therefore determining the mathematical form of *Φ(f)*. The successive approximations iteration becomes in this case a gradient

method with a fixed step (determined by time step ΔT) [11].

By means of minimizing the term $\|Cf\|^2$, a restored image is supposed to be gained [13].

Operator C is used to constrain the high frequency energy of the restored image. This leads to the restored image to be smooth.

On the other hand, the fidelity of the data is constrained with the following inequality:

$$\|g - h.f\|^2 \leq \epsilon^2 \tag{7}$$

Then, the condition for a minimum is that the gradient is equal to zero, and in this case will take the form:

$$\Phi(f) = (h^T h + \alpha C^T C)f - h^T g \tag{8}$$

Where $0.01 < \alpha < 1$.

Application of iteration in eq. (13) then the iterative least square will take the following form [11]:

$$f_{k+1} = f_k - \Delta T[(h^T h + \alpha C^T C)f_k - h^T g] \tag{9}$$

4.3 L^2 Norm Regularization Method:

It is also known as **Euclidean norm**. The Euclidean norm of a complex number is the absolute value (also called the **modulus**) of it. The L^2 norm has the property that it is continuously differentiable and is minimized by traditional linear optimization techniques, but it sacrifices the quality of the resulting image. This is due to the fact that it leads to non-directional regularizer that smooths the images blindly regardless of the existing edges [15].

The following equation explains how L^2 norm is used in order to estimate the latent image:

$$\hat{f} = argmin_f \{\tfrac{1}{2}\|Hf - g\|^2 + \lambda\|\nabla f\|^2\} \tag{10}$$

This equation can be re-written as follows:

$$f_{k+1} = f_k - \Delta T.\{h^T(h * f_k - g)\lambda\nabla f_k\} \tag{11}$$

4.4: Total Variation Regularization Method:

Total variation regularization is a non-quadratic measure that achieved popularity in recent years. **Regularization** is allowing the inclusion of prior knowledge to stabilize the solution in the presence of degradation sources -such as noise- and identifying physically meaningful and reasonable estimates [16]. The total-variation norm is a measure of the sum of the lengths of all the level lines in the image defined for discrete finite number of levels [15].

A regularization method is defined as an inversion method. This method depends on a single real parameter $\alpha \geq 0$. It leads to a family of approximates solutions $\hat{f}(\alpha)$ with **two properties**.

The **first property** is, for large enough α, the regularized solution $\hat{f}(\alpha)$ is stable in the face of disturbances or noise in the data.
The **second property** is, as α goes to zero the un-regularized generalized solution is recovered: $\hat{f}(\alpha) \to \hat{f}^{+}$ as $\alpha \to 0$.

The parameter α is called the "regularization parameter" and it controls the tradeoff between solution stability (i.e., noise propagation) and nearness of the regularized solution *f*(α) to the un-regularized solution f^{+} (i.e., approximation error in the absence of noise). Since the generalized solution represents the highest possible fidelity to the data, another way of viewing the role of α is in controlling the tradeoff between the impact of data and the impact of prior knowledge on the solution [12].

Let's consider this family of estimates that can be obtained as the solution of the following generalized equation:

$$\hat{f}(\alpha) = \arg\min J_1(f, g) + \alpha^2 J_2(f) \tag{12}$$

Where J_2 can be calculated from the following formulation:

$$J_2(f) = \|Df\|_1 = \sum_{i=1}^{N_f} |[Df]_i| \tag{13}$$

Combining eq. (12) and eq. (13) leads to a formulation of the total variation estimate:

$$\hat{f}_{TV}(\alpha) = \arg\min \|g - hf\|_2^2 + \alpha^2 \sum_{i=1}^{N_f} |[Df]_i| \tag{14}$$

This formulation can be re-written in a computational form as follows:

$$\hat{f}^{(i+1)} = f^i - \Delta T.h^T(f * h - g) - \lambda\zeta \quad (15)$$

5: Non-Blind Image Restoration: related work (past, present and future)

In kernel estimation, several participations were produced. Tanaka *et al.* [8] produced the Sinc function algorithm to compute the needed parameters (angle θ, distance *l*) for computing the kernel. Beimond *et al.* [10] and Krahmer *et al.* [9] used the Cepstrum of the blurred image to compute the angle of motion blur and the displacement.

Some researchers [2][6][7][17] found that by using the blurred image, and some prior information, the kernel can be estimated more accurately compared with the blind de-convolution techniques.
Shan *et al.* [17] introduced an approach for achieving a de-blurred image using a unified **probabilistic model** for estimating both blur kernel and the desired un-blurred image using **blind restoration**. They built a probabilistic model using $MAP_{f,h}$. In this approach, a pair of latent image *f* and kernel *h* is used to maximize the posterior probability given the observed blurred image *g*. The goal is to infer both *f* and *h* given a single input *g* [7]. The maximization of the posterior probability can be gained from the following formula shown in eq.(16):

$$p(f,h|g) \propto p(g|f,h)p(f)p(h) \quad (16)$$

The resulted de-blurred images were more accurate compared to parameter estimation techniques and some blind restoration techniques [17] but were not sufficient.
Levin *et al.* [7] proved that Shan's model like other blind restoration techniques using $MAP_{f,h}$ led to a deadlock as $MAP_{f,h}$ estimation encounters some limitations that lead to failure in estimating the latent image and the blurring kernel. The probability of the blurred image plus delta/identity kernel pair is higher than the probability of the sharp image with the correct kernel [2] as given in eq.(17).

$$P(g,h_\Delta) > P(\hat{f},\hat{h}) \quad (17)$$

Where h_Δ is a delta or identity (unit sample) kernel.

That means, if it is given an arbitrary large image *f* sampled exactly from a sparse prior and a blurred version *g*, then the explanation in which we set the image as the observed blurred image *g* and the kernel *h* as delta, is more probable than the correct explanation

with the true sharp image *f* and true kernel *h*. It means that the $MAP_{f,h}$ approach will always fail [7].

Levin *et al.* [7] reached that The failure of $MAP_{f,h}$ can be explained by the following reasons. **First**, the lack of measurements that are needed to estimate both kernel and the latent\de-blurred image leads to the inability to estimate the huge numbers of unknowns [18][19]. $MAP_{f,h}$ depends on the blurred image with the known of its size to estimate the unknowns of the latent image's size plus the unknowns of the kernel's size. **Second**, even with presence of a perfectly correct prior –which is not applicable– the $MAP_{f,h}$ fails to produce a successful estimate of both kernel and latent image. **Another effective reason** for $MAP_{f,h}$'s failure is the choice of the estimator. With the lack of the measurements and the favorability of the blur contents, a perfect estimator is needed in order to reduce the disadvantages' effects of the $MAP_{f,h}$.

In order to overcome that deadlock, Levin *et al.* [7] proposed that it will be sufficient to use MAP_h instead of $MAP_{f,h}$ and that leads to way back to non-blind restoration by separating the restoration process into two stages instead of one combined iterative stage as it is in blind restoration.
Therefore, in eq. (18), Krishnan *et al.* [2] and Levin *et al.* [7] proposed that the image gradients can be used as the prior information for estimating the kernel for regularization. Then, the resulted estimated kernel can be used in the second stage to de-blur the degraded image with a non-blind restoration technique.

$$\arg\max P(h|g) = \int P(f,h|g)df \tag{18}$$

Eq. (18) shows that there will be a lot of information depending on the size of the degraded image *g* to estimate -the much lesser in size- the kernel *h*. This will overcome a major obstacle meets $MAP_{f,h}$ in estimating kernel.

6: Discussions and Experimental Work:

In this section, we will discuss experimental work performed to compare between several image restoration algorithms to estimate the latent image by means of different kernel estimation approaches.
The kernel estimation approaches are ***parameter*** estimation approach (***Sinc*** function and ***Cepstral*** methods) and ***MAP*** estimation approach (Fergus and Krishnan estimation techniques).
The image restoration algorithms used to estimate the latent image are those algorithms discussed in section (4) (Least squares ***LS***, Constrained Least Squares ***CLS***, L^2 ***Norm***, Total Variation ***TV***) and added to them the famous Lucy-Richardson ***L-R***.

Two types of images were used in these experiments. Those types can be classified into images suffering synthetic blur and images suffering real blur.
Several measuring merits were used compute the efficiency of the image restoration algorithms when used with different kernel estimation approaches in different cases of linear motion blurs. Those measuring merits are Peak Signal-to-Noise Ratio ***PSNR***, Normalized Mean Square Error ***NMSE***, and Maximum Absolute Error. In PSNR comparison, as the result ratio goes higher, the success of the restoration algorithm becomes better. While in both NMSE and Maximum Absolute Error, as the result ratio becomes lesser, the success of the restoration algorithm becomes better.

Experiment 1: Those images used in this experiment were degraded by means of synthetic linear motion bur with angle θ=30 and displacement l=5, 10, 15, 20. Figure (5) shows Image samples used in the experiments for kernel estimation approaches and restoration algorithms evaluation.
The time consuming of the ***Sinc function*** was taken in consideration so that the degree of blur were chosen as an integer degree. Also the image samples were used with noise free.
After analyzing the results computed using the different used restoration techniques with the used kernel estimation methods over images degraded with synthetic blur (table 1- figure 7), we can conclude that:

- The Total variation ***TV*** restoration technique with the ***Sinc function*** kernel estimation methods gives better results among the different kernel estimation techniques.
- The ***L^2 Norm*** restoration technique with the ***Krishnan*** kernel estimation method gives a good result when comparing the two MAP kernel estimation approach's method.
- The ***Cepstral*** kernel estimation method estimates the angle θ of the linear motion blur very close to but does not give the exact angle due to the calculation methods. This calculation method depends on the position of the two peaks in a matrix of 256x256 or 512x512 of the FFT of the blurred matrix (see figure 3).
- The ***Sinc function*** kernel estimation method is a highly timing consuming technique specially when dealing with fractions of angles.

Experiment 2: For more accurate evaluation, extended experiments were applied for image samples degraded with real blur. Figure (6) shows Image samples used in these experiments.
After analyzing the results computed using the different used restoration techniques with the used kernel estimation methods over images degraded with real blur (table 2- figure 8), we can conclude that:

- The parameter estimation techniques used for kernel estimation failed to introduce an acceptable estimate for the desired kernel. These techniques were built depending on the linearity of the kernel.
- The kernels estimated by MAP kernel estimation approaches (figure 9) show that in real life, there is no linearity in the kernel causing blurriness due to linear motion. This comes from the interference of other circumstances in the real life.
- The ***Total Variation*** then ***L-R*** restoration algorithms give best results compared with the other algorithms used in this experiment.
- The Krishnan's kernel estimation algorithm produces more successful results compared Fergus' algorithm.
- The key of obtaining a better estimated latent image is the use of the right estimator to be used in a MAP kernel estimation approach.

(a) Original images (baboon, kid, and fishing boat)

(b) Blurred image with θ=30 and l=20

Figure (5): *Image samples used in experiment (1) for kernel estimation approaches and restoration algorithms evaluation: (a) Original images. (b) Images degraded by synthetic blur with angle θ=30 and displacement l=20.*

7: Conclusions and Future Work:

According to the discussions and the experimental work, we can conclude that:

-The parameter estimation techniques are not sufficient to get an estimate for the kernel caused the blurriness. It can work with images degraded with synthetic blur but it fails with images suffering real blur.

- Although that ***Total Variation*** restoration algorithm gives better results, but it is noticed that all the restoration techniques produced acceptable results. Since the number of the unknowns in the kernel is much less than the number of known information in the degraded images, a good estimate of the kernel would be reachable. With the help of that good kernel estimation, a good result can be achieved using any restoration algorithm.

-As a future work, the research of the MAP_h kernel estimation approach can be extended by producing a successful estimator to improve the output of these approaches and compare this output by using several image restoration techniques.

Figure (6): *Real blurred image samples used in experiment (2) for kernel estimation approaches and restoration algorithms evaluation.*

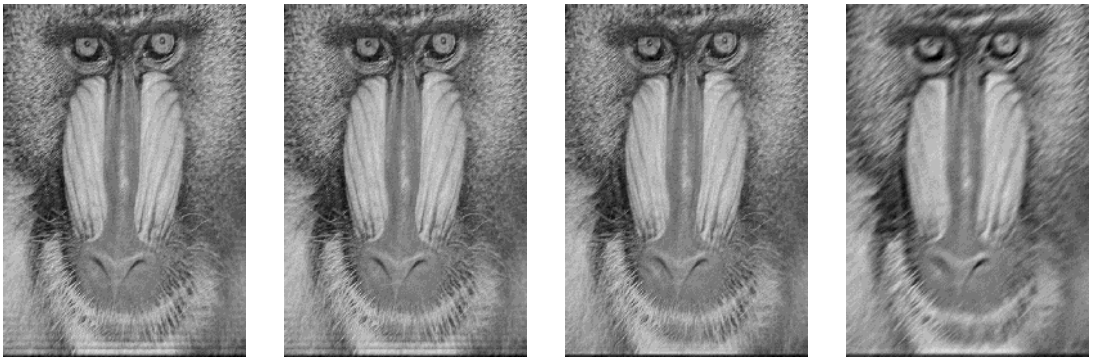

(a) Testing results of baboon by Sinc function, Cepstral, Fergus and Krishnan kernel estimation algorithms respectively.

(b) Testing results of kid by Sinc function, Cepstral, Fergus and Krishnan kernel estimation algorithms respectively.

(c) Testing results of fishing boat by Sinc function, Cepstral, Fergus and Krishnan kernel estimation algorithms respectively.

***Figure (7)** Results of the kernel estimation and the restitution process for images degraded by synthetic blur with angle $\theta=30$ and displacement $l=20$.*

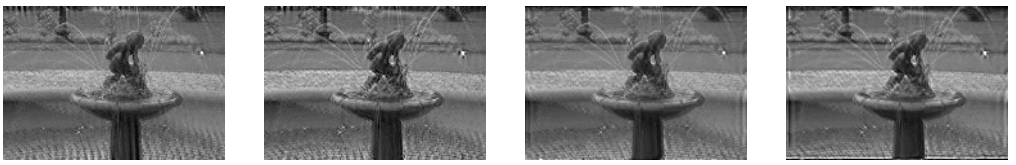

(a) *Testing results of fountain by Fergus' and Krishnan kernel estimation algorithm with L-R then by Total Variation restoration algorithms respectively.*

(b) *Testing results of statue by Fergus' and Krishnan kernel estimation algorithm with L-R then by Total Variation restoration algorithms respectively.*

(c) Testing results of fishes by Fergus' and Krishnan kernel estimation algorithm with L-R then by Total Variation restoration algorithms respectively.

Figure (8): *Results of the kernel estimation and the restitution process for images degraded by real blur.*

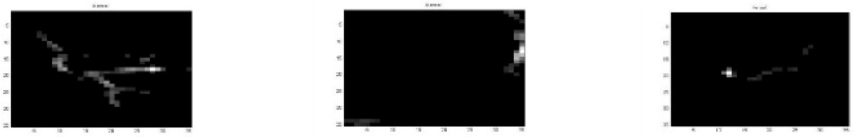

(a) Kernels estimated by Fergus' algorithm for fountain, lyndsey, and fishes respectively.

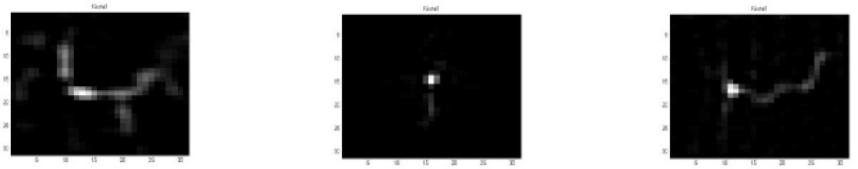

(b) Kernels estimated by Fergus' algorithm for fountain, lyndsey, and fishes respectively.

Figure (9): *The output of MAP_h kernel estimation approach's techniques.*

Table (1): PSNR testing Experimental Results for synthetic blurred samples.

		baboon				kid				fishingboat			
		Parameter est.		MAP est.		Parameter est.		MAP est.		Parameter est.		MAP est.	
		Sinc	Cepstral	Fergus	Krishnan	Sinc	Cepstral	Fergus	Krishnan	Sinc	Cepstral	Fergus	Krishnan
Length = 5	L. S.	25.16492	25.046	20.85242	20.81114	33.30956	33.86511	30.02822	28.29673	29.30262	29.25953	26.12637	25.01253
	C.L.S.	25.32834	24.7633	21.20514	21.18311	33.69998	34.25164	30.12373	27.95094	30.14736	30.36164	26.11498	24.84737
	L2 Norm	23.88298	23.7713	21.4545	22.05851	32.81922	33.08525	30.21824	30.08839	28.7458	28.76466	26.17624	26.10693
	T.V.	27.97509	26.44143	20.72714	20.38016	33.60577	35.47268	29.53843	28.41357	31.00937	31.97291	25.91988	24.63174
	L-R	25.09193	24.02571	20.35321	20.10209	32.23028	30.5393	28.9725	26.72897	29.37184	29.56297	25.49126	24.06318
Length = 10	L. S.	22.58218	22.56243	19.19213	20.34644	30.34839	30.06731	25.12148	27.11726	26.06148	25.81147	26.06191	23.49479
	C.L.S.	23.31031	23.2879	19.15984	19.87355	32.81507	31.65643	24.8217	26.96222	28.54556	27.56684	28.17847	22.8154
	L2 Norm	21.87831	21.87188	19.66403	20.88706	29.99995	29.85152	25.35999	28.33929	25.76288	25.62671	25.77837	24.14664
	T.V.	25.26192	25.20132	18.7787	19.42641	34.39888	32.04019	24.62388	27.70258	30.1771	28.12881	29.06424	22.65528
	L-R	22.62097	22.61293	18.55716	19.51639	28.11554	28.38714	24.38852	25.50227	25.38325	25.40002	25.28113	22.64558
Length = 15	L. S.	21.58083	21.11041	19.92083	20.16327	28.69708	28.64446	24.85292	26.73116	24.74591	24.49084	23.02145	22.83647
	C.L.S.	22.00051	21.40027	20.12366	19.47965	31.42719	31.34455	24.44324	26.90772	27.11631	25.8398	23.27608	22.08166
	L2 Norm	21.1306	20.94064	20.1505	20.38813	28.45419	28.40808	25.06227	27.46549	24.50451	24.3349	23.07949	23.18248
	T.V.	23.62964	21.20896	19.89658	19.3845	32.55898	32.37683	24.37199	27.59749	28.41481	26.17384	23.09498	21.95361
	L-R	21.40625	20.56441	19.32829	19.34739	26.34649	26.3975	23.99739	24.64367	23.67992	23.1807	21.88702	22.11079
Length = 20	L. S.	23.7856	23.80128	23.2722	22.40282	27.53709	27.41759	25.78189	26.19559	23.7856	23.80128	23.2722	22.40282
	C.L.S.	25.77978	25.88305	23.96212	21.75289	30.28502	29.83319	24.70092	26.60698	25.77978	25.88305	23.96212	21.75289
	L2 Norm	23.61628	23.62568	23.21803	22.64072	27.34762	27.26313	25.89549	26.69426	23.61628	23.62568	23.21803	22.64072
	T.V.	26.97866	27.08326	24.11333	21.7123	31.06008	30.25232	24.59611	27.2588	26.97866	27.08326	24.11333	21.7123
	L-R	22.71279	22.65545	21.87613	21.57437	25.36609	25.31816	24.14156	24.02416	22.71279	22.65545	21.87613	21.57437

Table (2): Experimental Results testing real-blurred images.

			L. S.	C.L.S.	L2 Norm	T.V.	L-R
Fountain	Std. Dev.	Fergus	2.771363	3.308195	2.739454	3.41934	3.165174
		Krishnan	2.827855	3.397921	2.762944	3.439504	3.636333
	Entropy	Fergus	6.993518	7.094207	6.958414	7.120901	7.115927
		Krishnan	7.034619	7.146747	6.994677	7.172354	7.172404
Lyndsey	Std. Dev.	Fergus	6.92772	6.841682	6.657381	6.967482	6.723073
		Krishnan	6.70691	6.574094	6.350984	6.76003	6.653942
	Entropy	Fergus	6.11875	6.114636	6.143836	6.086975	6.107174
		Krishnan	6.149692	6.149255	6.13035	6.150782	6.139687
Fishes	Std. Dev.	Fergus	5.874557	5.871465	5.889488	5.851086	6.588245
		Krishnan	6.012697	6.111344	5.961051	6.079441	7.239815
	Entropy	Fergus	7.313567	7.321651	7.29558	7.336833	7.354114
		Krishnan	7.444771	7.500474	7.39646	7.530764	7.528223

References

[1] R. Fergus, B. Singh, A. Hertzmann, S.T. Roweis, and W.T. Freeman, "Removing camera shake from a single photograph", SIGGRAPH,(2006).

[2] Dilip Krishnan, Terence Tay, and Rob Fergus, “Blind Deconvolution using a Normalized Sparsity Measure”, IEEE Conf. on Computer Vision and Pattern Recognition CPVR, (2011).

[3] D. Kundur and D. Hatzinakos, “Blind image de-convolution”, *IEEE Signal Process. Mag.* 13,43-64, (1996).

[4] M. R. Banham and A. K. Katsaggelos, "Digital image restoration",Signal Processing Magazine, IEEE, 14(2):24–41, (1997).

[5] Reginald L. Lagendijk and Jan Biemond, “Basic Methods for Image Restoration and Identification”, Al Bovik, “Handbook of Image and Video Processing”, Academic Press, Second Edition,ISBN 978-0-12-119792-6, (2005).

[6] J. W. Miskin and D. J. C. MacKay, "Ensemble learning for blind image separation and deconvolution", In Advances in Independent Component Analysis, Springer, (2000).

[7] Anat Levin, Yair Weiss, Fredo Durand, and William T. Freeman, “Understanding and Evaluating Blind Deconvolution Algorithms”, IEEE Conf. on Computer Vision and Pattern Recognition, (2009).

[8] Masayuki Tanaka, Kenichi Yoneji, and Masatoshi Okutomi, “Motion Blur Parameter Identification from a Linearly Blurred Image ”, Paper on ICCE, (2007).

[9] Felix Krahmer, Youzuo Lin, Bonnie McAdoo, Katharine Ott, Jiakou Wang, David Widemann, Mentor: Brendt Wohlberg, "Blind Image Deconvolution: Motion Blur Estimation", Technical Report, Institute of Mathematics and Applications, University of Minnesota, (2006).

[10] J. Biemond, R L. Lagendijk, and R M. Mersereau, "Iterative methods for image deblurring", *Proc. IEEE* 78,856-883, (1990).

[11] Aggelos K. Katsaggelos, and Chun-Jen Tsai, "Iterative Image Restoration", Al Bovik, "Handbook of Image and Video Processing", Academic Press, Second Edition,ISBN 978-0-12-119792-6, (2005).

[12] William C. Karl, "Regularization in Image Restoration and Reconstruction", Al Bovik, "Handbook of Image and Video Processing", Academic Press, Second Edition,ISBN 978-0-12-119792-6, (2005).

[13] B. R. Hunt, "The Application of constrained least squares estimation to image restoration by digital computers", IEEE Trans. Comput. C-22,805-812, (1973).

[14] A. N. Tikhonov and V. Y. Arsenin, "Solution of ill-posed problems", Willy–Winston, (1977).

[15] Hussein A. Aly, " Regularized Image Up-sampling", Ph.D. Thesis, University of Ottawa, (2003).

[16] M. Bertero, "Linear inverse and ill-posed problems", in advances in Electronics and Electron physics (Academic, New York), Vol. 75, (1989).

[17] Qi Shan, Jiaya Jia, and Aseem Agarwala, "High-quality Motion Deblurring from a Single Image", ACM Transactions on Graphics, Vol. 27, (2008).

[18] S. M. Kay, "Fundamentals of Statistical Signal Processing: Estimation Theory", Prentice Hall, (1997).

[19] D. Brainard and W. Freeman, "Bayesian color constancy" , JOSA A, Vol. 14, Issue 7, pp. 1393-1411, (1997).

Nomenclatures:

f …	The latent image.
h …	The blur kernel (PSF).
n …	The added noise.
$\otimes$ …	Mathematical operator denoting for the convolution process.
Φ…	The circular convolution shift.
k…	The iteration processed number.
β…	Relaxation parameter.
I…	Identity matrix.
$.^T$…	The transpose of a matrix.
C…	High pass operator.
α…	Regularization parameter.
ΔT…	The time step.
∇f…	The spatial gradient of f.
J_1…	General distance measure between the data and the its prediction based on the estimated f.
J_2...	General regularizing penalty.
$\|.\|_1$…	Sum of absolute value of the elements (L^1 norm).
D…	Discrete approximation to the gradient operator.
N_f...	Length of vector f.
ζ...	Image curvature (Laplacian derivative operator).
h_Δ…	Delta or identity (unit sample) kernel.